

Turbulent Kinetic Energy Assessed by Multipoint 4-Dimensional Flow Magnetic Resonance Imaging Provides Additional Information Relative to Echocardiography for the Determination of Aortic Stenosis Severity

Christian Binter, PhD*; Alexander Gotschy, MD, MSc*; Simon H. Sündermann, MD; Michelle Frank, MD; Felix C. Tanner, MD; Thomas F. Lüscher, MD; Robert Manka, MD; Sebastian Kozerke, PhD

Background—Turbulent kinetic energy (TKE), assessed by 4-dimensional (4D) flow magnetic resonance imaging, is a measure of energy loss in disturbed flow as it occurs, for instance, in aortic stenosis (AS). This work investigates the additional information provided by quantifying TKE for the assessment of AS severity in comparison to clinical echocardiographic measures.

Methods and Results—Fifty-one patients with AS (67±15 years, 20 female) and 10 healthy age-matched controls (69±5 years, 5 female) were prospectively enrolled to undergo multipoint 4D flow magnetic resonance imaging. Patients were split into 2 groups (severe and mild/moderate AS) according to their echocardiographic mean pressure gradient. TKE values were integrated over the aortic arch to obtain peak TKE. Integrating over systole yielded total TKE_{sys} and by normalizing for stroke volume, normalized TKE_{sys} was obtained. Mean pressure gradient and TKE correlated only weakly ($R^2=0.26$ for peak TKE and $R^2=0.32$ for normalized TKE_{sys}) in the entire study population including control subjects, while no significant correlation was observed in the AS patient group. In the patient population with dilated ascending aorta, both peak TKE and total TKE_{sys} were significantly elevated ($P<0.01$), whereas mean pressure gradient was significantly lower ($P<0.05$). Patients with bicuspid aortic valves also showed significantly increased TKE metrics ($P<0.01$), although no significant difference was found for mean pressure gradient.

Conclusions—Elevated TKE levels imply higher energy losses associated with bicuspid aortic valves and dilated ascending aortic geometries that are not assessable by current echocardiographic measures. These findings indicate that TKE may provide complementary information to echocardiography, helping to distinguish within the heterogeneous population of patients with moderate to severe AS. (*Circ Cardiovasc Imaging.* 2017;10:e005486. DOI: 10.1161/CIRCIMAGING.116.005486.)

Key Words: 4D flow magnetic resonance imaging ■ aortic dilation ■ aortic stenosis ■ bicuspid aortic valve ■ echocardiography ■ magnetic resonance imaging ■ turbulent kinetic energy

Aortic stenosis (AS) is the most prevalent valvular heart disease in adults of advanced age and, if untreated, is associated with a high mortality when symptoms occur.^{1,2} According to current guidelines, the diagnosis of severe AS is based on echocardiographic measures of mean pressure gradient (MPG) and aortic valve effective orifice area (AVA).^{3,4} Class I indications for valve replacement are severe, symptomatic AS or severe AS with reduced left ventricular ejection fraction.^{3,4} However, gauging symptoms of AS is highly subjective and can be confounded by various other diseases: for example, coronary artery disease, pulmonary disease, or orthopedic disorders. In addition, correct quantification of

AS severity by 2-dimensional (2D) echocardiography is challenging, and AS severity is misclassified in a non-negligible portion of the patient population.^{5–8} This misclassification has in part been associated with the effect of pressure recovery and its dependence on valve morphology and ascending aortic (AAo) diameter, which is not accounted for in standard echocardiographic metrics.

See Editorial by von Knobelsdorff-Brenkenhoff See Clinical Perspective

An echocardiographic approach to correct for pressure recovery is the energy loss index (ELI),⁹ which represents

Received August 5, 2016; accepted April 21, 2017.

From the Institute for Biomedical Engineering, University and ETH Zurich, Switzerland (C.B., A.G., S.K.); Department of Cardiology, University Heart Center (A.G., M.F., F.C.T., T.F.L., R.M.), Division of Internal Medicine (A.G.), and Institute of Diagnostic and Interventional Radiology (R.M.), University Hospital Zurich, Switzerland; Department of Cardiothoracic and Vascular Surgery, Deutsches Herzzentrum Berlin, Germany (S.H.S.); and Imaging Sciences and Biomedical Engineering, King's College London, United Kingdom (S.K.).

*Drs Binter and Gotschy share first authorship.

The Data Supplement is available at <http://circimaging.ahajournals.org/lookup/suppl/doi:10.1161/CIRCIMAGING.116.005486/-/DC1>.

Correspondence to Sebastian Kozerke, PhD, Institute for Biomedical Engineering, University and ETH Zurich, Gloriastrasse 35, 8092 Zurich, Switzerland. E-mail kozerke@biomed.ee.ethz.ch

© 2017 American Heart Association, Inc.

Circ Cardiovasc Imaging is available at <http://circimaging.ahajournals.org>

DOI: 10.1161/CIRCIMAGING.116.005486

an advancement of AVA measurement because it adjusts the AVA for the hemodynamic effect of flow expansion by taking into account the diameter of the sinotubular junction (STJ). In vitro and in vivo catheter-based measurements of AS severity showed a better correlation with ELI than with AVA.¹⁰ In addition, ELI has shown independent and additional prognostic information to that derived from conventional echocardiographic measures of AS severity¹¹ and is therefore regarded as the most accurate measurement of AS in terms of flow in the current echocardiographic guidelines.¹² However, AS also causes abnormal blood flow patterns in the AAO, which have been shown to significantly influence left ventricular remodeling.¹³ Those aortic flow patterns and differences in valve morphology are not factored in when computing the ELI. Furthermore, a limited acoustic window or an eccentric jet can hamper a parallel alignment of the echo beam with the flow jet, which in turn compromises the accuracy of ELI and classical measures of AS severity.

Phase-contrast magnetic resonance imaging (MRI)^{14–16} allows to acquire time-resolved velocities and directions of blood flow within the entire aortic arch (4D flow MRI).^{14–16} Four-dimensional flow MRI also enables direct investigation of the mechanisms responsible for energy dissipation.^{17,18} In particular, the assessment of turbulent kinetic energy (TKE)—the energy stored in turbulent flow—enables gauging energy losses caused by AS¹⁹ because TKE is largely dissipated into heat. TKE can be quantified operator independently and reproducibly by 4D flow MRI, and it has been shown that TKE correlates with irreversible pressure loss as evidenced in a pilot study.²⁰ Ha et al²¹ recently validated MRI-based TKE measurements against particle tracing velocimetry in vitro. In vivo, however, the same study observed inconsistencies between MRI-based TKE and echocardiographic transvalvular pressure gradient measurements in a case series of 7 patients with various valvular diseases and 1 healthy control. Accordingly, the clinical value of TKE for the assessment of AS and its relation to echocardiographic MPG and ELI is yet unknown.

In this study, we investigated whether TKE derived from 4D flow MRI correlates with echocardiographic measures for the determination of AS severity or provides independent and complementary information.

Methods

Study Design

Between September 2012 and November 2014, 55 patients with AS (67±15 years, 20 female), referred to the local echocardiography laboratory, and 10 healthy, age-matched controls (69±5 years; 5 female) were prospectively enrolled. Exclusion criteria were an ejection fraction <50%, significant disease of any other valve, severe aortic regurgitation, and the standard exclusion criteria for MRI.²²

The study was approved by institutional and local ethics committees. Written informed consent was obtained from all study subjects before examination. All subjects underwent a 4D flow MRI examination in addition to a routine cardiac MRI protocol for the assessment of cardiac function and aortic geometry. Furthermore, all AS patients had a routine echocardiography examination performed. Median time difference between the examinations was 14 days (25th and 75th percentiles: 2 and 30 days, respectively).

MRI Data Acquisition

All MRI data were acquired on a clinical 3 T scanner (Philips Healthcare, Best, The Netherlands). To obtain 4D flow MRI data for the calculation of TKE maps, a spoiled gradient echo sequence with 10 different velocity encodings (3 per spatial direction plus 1 reference encoding) was used. This multipoint velocity encoding strategy (multipoint 4D flow MRI) was combined with Bayesian data processing,^{23,24} improving the dynamic range of previous single velocity encoding approaches.^{20,21} For each direction, the velocity encoding values were set to 450, 150, and 50 cm/s for patients and 200, 67, and 40 cm/s for the control group. Prospective cardiac triggering and respiratory navigator-based gating allowed for acquisition during free-breathing with an isotropic spatial resolution of 2.5×2.5×2.5 mm³ and a heart rate-dependent temporal resolution of 22 to 44 ms. The field of view (238–440×240–300×47.5–80 mm³) was adjusted for each subject to cover the aortic root and the aortic arch. The acquisition was accelerated using 8-fold k-t PCA²⁵ with a net acceleration factor of 7.1, resulting in a total scan time of 17.2±4.7 minutes depending on navigator efficiency. With this setup, an average signal-to-noise ratio of 20 in the AAO was obtained. Additional details can be found in the [Data Supplement](#).

MRI Data Processing and TKE Calculation

Multipoint 4D flow MRI data were reconstructed using a custom-made software implemented in Matlab (MathWorks, Natick, MA). Data were corrected for concomitant gradient field effects. Background phase errors were compensated by fitting a plane to the phase of static tissue.^{26–29} Subsequently, Bayesian processing was performed to simultaneously calculate mean velocities and intensities of velocity fluctuations per image voxel along each velocity encoding direction and for each time point in the cardiac cycle. Voxelwise TKE values were then computed according to¹⁷:

$$\text{TKE} \left[\frac{\text{J}}{\text{m}^3} \right] = \frac{\rho}{2} \sum_{i=1}^3 \sigma_i^2 \quad (1)$$

where σ_i^2 is the variance of the velocity fluctuations for direction i , and ρ is the blood density, assumed to be 1060 kg/m³.

MRI Data Analysis

Data analysis was performed by 2 blinded readers (C.B., A.G.) with 5 and 6 years of experience in MRI. For the TKE analysis, the thoracic aorta was segmented semiautomatically to obtain the investigation domain, which included the AAO, aortic arch, and descending aorta up to the level of the right pulmonary artery. TKE was integrated over the entire investigation volume for each time frame. For analysis, the values for peak systole (peak TKE) and values integrated over systole (total TKE_{sys}) are reported.

To normalize TKE with respect to the hemodynamic work of the heart per beat, total TKE_{sys} was related to the stroke volume (SV):

$$\text{Normalized TKE}_{\text{sys}} \left[\frac{\text{mJ}}{\text{mL}} \right] = \frac{\text{Total TKE}_{\text{sys}}}{\text{SV}} \quad (2)$$

This value refers to the amount of dissipated TKE per milliliter stroke volume and represents an indicator for the efficiency of the heart. To display the flow fields, pathline visualization was performed with GTFlow (GyroTools LLC, Zurich, Switzerland). The pathlines were emitted from 4 planes spaced evenly along the AAO during the first 200 ms of systole. The velocity field was masked to illustrate the volume of interest for the TKE calculations. More detailed information on MRI data analysis and reproducibility is given in the [Data Supplement](#).

Echocardiographic Measurements

To obtain the left ventricular outflow tract and transaortic flow velocity profiles, pulsed wave Doppler for the left ventricular outflow tract and continuous wave Doppler data for transaortic flow were recorded.

MPG was calculated using the modified Bernoulli equation as recommended in current guidelines.¹² For determination of ELI, AVA was calculated by the continuity equation. In addition, the diameter of the AAO at the level of the STJ was measured inner edge-to-inner edge as the only parameter reflecting the AAO geometry. The cross-sectional area (AA) of the STJ was derived from the aortic diameter. With this data, the ELI, indexed to body surface area, was computed according to Garcia et al⁹:

$$ELI \left[\frac{cm^2}{m^2} \right] = \left(\frac{AVA \cdot AA}{AA - AVA} \right) \cdot \frac{1}{BSA} \quad (3)$$

Statistical Analysis

Continuous and categorical data are expressed as mean±SD or as a percentage, respectively. Continuous data were evaluated with 1-way ANOVA and Holm–Bonferroni post hoc test. To analyze the effect of bicuspidity and aortic dilatation and their interaction on energy loss in the AS patient group, a 2-way ANOVA was performed. Homogeneity of variance was tested by a Levene test and a logarithmic transform was applied when appropriate. For comparison of categorical data, a binomial test was used. Correlation was investigated using linear regression. Values of $P < 0.05$ were considered statistically significant; all statistical tests were 2-sided and performed in R (R v3.2.2; R Foundation for Statistical Computing, Vienna, Austria).

Results

Patient Characteristics

Data acquisition and evaluation was successful in 51 of the 55 enrolled patients (93%) and in all 10 controls. One scan had to be aborted because of patient discomfort/claustrophobia, 2 examinations could not be evaluated because of breathing artifacts or lack of compliance, and 1 examination was excluded because of incomplete coverage of the aortic arch. Thirty-one male (61%) and 20 female patients with a mean age of 67±15 years were finally included in the analysis. According to echocardiographic measures, 27 patients had severe AS (MPG ≥40 mmHg), and 24 patients had mild/moderate AS (MPG <40 mmHg). Dilatation of the AAO, defined as AAO diameter ≥4.0 cm as determined by echocardiography, was found in 15 patients, and 11 patients exhibited bicuspid aortic valve morphology. All healthy controls exhibited normal aortic diameter and tricuspid valve morphology. In 48 of the final 51 patients, ELI could be determined, 3 data sets had to be excluded from the ELI analysis because of insufficient or unavailable data. The total sex distribution of the patients without subgroups (60.7% male) did not significantly differ ($P=0.16$) from the control group (50% male). Furthermore, there was no significant difference in MPG, peak TKE, or normalized TKE_{sys} between male and female controls ($P=0.32$, 0.77, or 0.68, respectively). Table 1 provides an overview of the baseline characteristics of patients and healthy controls.

Comparison of MRI-Based TKE Between AS Patients and Controls

Peak TKE, total TKE_{sys}, and normalized TKE_{sys} were evaluated in all study subjects. The reference values, measured in healthy controls, were peak TKE 4.8±1.0 mJ, total TKE_{sys} 20.6±4.1 mJ, and normalized TKE_{sys} 0.32±0.07 mJ/mL. All 3 parameters were found to be highly significantly elevated in patients with AS (peak TKE, 25±10 mJ, $P<0.001$; total TKE_{sys}, 90±37 mJ, $P<0.001$; and normalized TKE_{sys} 1.23±0.57

Table 1. Overview of the Study Population

	Group 1, Severe AS	Group 2, Mild/Moderate AS	Controls	P Value
n	27	24	10	...
Male	12 (44%)*	19 (79%)†	5 (50%)	<0.0001
Female	15 (56%)*	5 (21%)†	5 (50%)	
Age, y	70±12	64±17	69±5	0.24
Body surface area, m ²	1.87±0.22	1.87±0.20	1.91±0.19	0.89
Indexed left ventricular mass, g/m ²	76±23	68±12	n/a	0.14
Systolic blood pressure, mm Hg	147±20*	133±21	134±9	0.045
Diastolic blood pressure, mm Hg	78±9	78±15	84±6	0.42
Aortic valve area, cm ²	0.73±0.16*†	1.25±0.28†	3.05±0.65	<0.0001
Diameter ascending aorta, cm	3.54±0.46*	3.9±0.51†	3.49±0.19	0.01
Diameter ≥4 cm	4 (15%)*	11 (46%)	...	0.0008
Bicuspid aortic valve	5 (19%)	6 (25%)	...	NS
Ejection fraction, %	63±7	61±5	n/a	NS

Data are mean±SD or number of patients (%). Aortic valve effective orifice area values determined using echocardiography for AS patients and magnetic resonance imaging for controls. AS indicates aortic stenosis; n/a, not available; and NS, not significant.

*Significant difference vs group 2.

†Significant difference vs healthy controls.

mJ/mL, $P<0.001$). However, between the patient groups with echocardiographic severe and mild/moderate AS, no significant difference of peak TKE and total TKE_{sys} was found, and only normalized TKE_{sys} was significantly higher in patients with MPG ≥40 mmHg when compared with those <40 mmHg (severe AS: normalized TKE_{sys} 1.34±0.53 mJ/mL versus mild/moderate AS: 1.1±0.6 mJ/mL; $P=0.02$). Table 2 lists the results of the TKE-based parameters of the different groups.

Correlation of MRI-Based TKE With Echocardiographic MPG and ELI

The relations between MPG and peak TKE and MPG and normalized TKE_{sys} are illustrated in Figure 1. A significant but weak correlation between TKE and MPG was found in the entire study population (peak TKE versus MPG: $R^2=0.26$, $P<0.0001$; normalized TKE_{sys} versus MPG: $R^2=0.32$, $P<0.0001$). No significant correlation was found if the control group was not included in the analysis.

The ELI metric negatively correlated with MPG ($R^2=0.49$, $P<0.0001$); however, it did neither correlate with peak TKE nor with normalized TKE_{sys} ($P=0.48$ and $P=0.96$, respectively). In 37% of the patient population, assessment of AS severity by TKE did not conform with the echocardiographic

Table 2. Results of the TKE-Based Parameters

	Group 1, Severe AS (MPG \geq 40 mmHg)	Group 2, Mild/Moderate AS (MPG <40 mmHg)	Group 3, Healthy Controls	P Value
Peak TKE, mJ	26.1 \pm 9.9*	24.5 \pm 10.5*	4.8 \pm 1.0	<0.001
Total TKE _{sys} , mJ	95 \pm 39*	83 \pm 35*	20.6 \pm 4.1	<0.001
Normalized TKE _{sys} , mJ/mL	1.34 \pm 0.53*†	1.10 \pm 0.60*	0.32 \pm 0.07	<0.001

Data are mean \pm SD. AS indicates aortic stenosis; MPG, mean pressure gradient; and TKE, turbulent kinetic energy.

*A significant difference vs healthy controls (P <0.001).

†A significant difference vs group 2 (P <0.05).

examination based on MPG (19 of 51 patients, yellow fields in Figure 1B). In the majority of cases (31%, 16 of 51 patients), 4D flow MRI revealed only moderate elevation of TKE, whereas echocardiography showed severe elevation of MPG.

To investigate potential causes for the weak correlation between MPG or ELI on the one hand and TKE on the other hand, the flow patterns and TKE distributions within the aortae were visualized. Figure 2 displays the flow patterns and TKE distributions of 3 selected patients. All patients had tricuspid valves, and the AAO of patient A was dilated (4.7 cm diameter). In Figure 2A and 2B, data of patients with comparable MPG transitioning to severe AS are shown. Patient A had an MPG of 35 mmHg, peak TKE of 53 mJ, and a normalized TKE_{sys} of 3.3 mJ/mL, whereas patient B had an MPG of 40 mmHg, peak TKE of 16 mJ, and a normalized TKE_{sys} of 0.8 mJ/mL. It is noted that TKE occurs in a large portion of the aortic arch in patient A, whereas in patient B, elevated TKE is limited to a small region distal to the aortic valve. Figure 2C depicts data of a patient with echocardiographic very severe AS (MPG of 74 mmHg) but only moderately elevated TKE. Here, again high TKE values are confined to the region of the

flow jet. Of note, patient C was asymptomatic and reported excellent physical fitness. Videos of the flow patterns of the 3 patients are available in the [Data Supplement](#). In patient C, the poststenotic accelerated flow continues unhindered to the descending aorta, whereas in patient A, the flow jet dissolves into pronounced flow disturbances in the AAO.

Influence of Valve Morphology and AAO Diameter

The group of patients with dilated AAO showed significantly lower MPG values (P =0.03) compared with patients with normal AAOs. The echocardiographic determination of the ELI, which accounts for AVA and the aortic diameter at the STJ, exhibited no significant difference between patients with dilated and normal AAO (P =0.06). In contrast, 4D flow MRI documented increased energy loss in this patient cohort with significantly elevated peak TKE but nonsignificantly elevated normalized TKE_{sys} values (P =0.002 and P =0.19 for peak TKE and normalized TKE_{sys}, respectively) compared with the normal aorta group (Figure 3).

Patients with bicuspid aortic valves had MPG (P =0.90) and ELI (P =0.61) values similar to those observed in patients with tricuspid aortic valves. However, peak TKE and normalized TKE_{sys} were found to be significantly higher in patients with a bicuspid aortic valve (P =0.0002 and P =0.003, respectively). No significant interaction of bicuspidity and aortic dilatation was seen for the TKE parameters. A graphical comparison between the groups can be found in Figure 4. An overview of all results is given in Table 3.

Discussion

This work has evaluated TKE derived from multipoint 4D flow MRI as a measure to gauge energy loss in patients with AS. The correlation of TKE metrics with established echocardiography-based measures of AS severity was investigated. Furthermore, we studied the factors that may account for discrepancies between TKE and echocardiographic parameters.

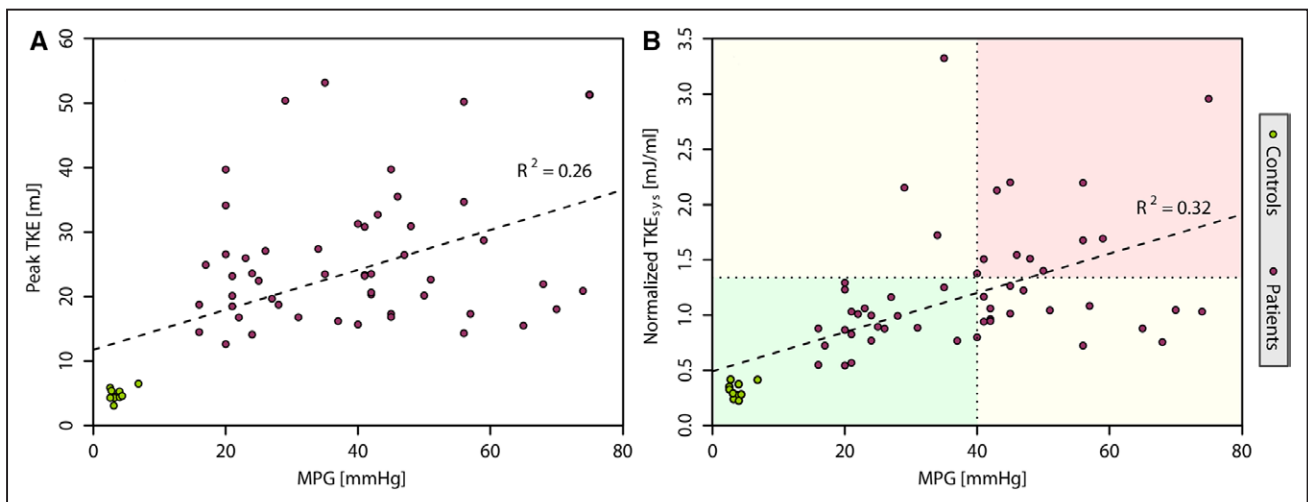


Figure 1. Correlation of mean pressure gradient (MPG) vs peak turbulent kinetic energy (peak TKE; **A**) and normalized TKE_{sys} (**B**). A significant but weak correlation is found for the entire study population, including both patients and controls. Within the patient group MPG and TKE are not correlated. On the right, a possible stratification scheme is outlined: in the green and red sector, MPG and normalized TKE_{sys} are in agreement and patients can be classified accordingly; in the yellow sectors, the discrepancy between energy loss and MPG implies that considering solely the MPG might result in a misleading classification. The limit for normalized TKE_{sys} was chosen as the average over the healthy controls plus 1.64 SD of the study population, representing the upper 95% quantile.

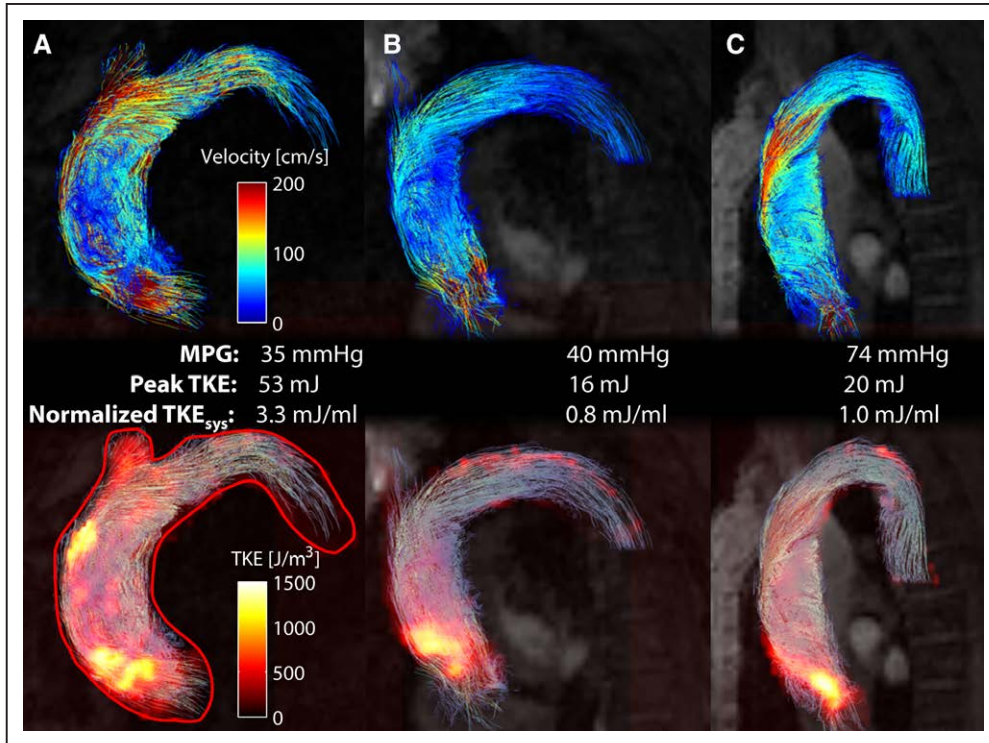


Figure 2. Pathlines (upper) and turbulent kinetic energy (TKE) maps (lower) for 3 exemplary patients. In **A** and **B**, patients A (male, 59 y) and B (female, 79 y) showed similar mean pressure gradient (MPG) but contrasting TKE values, whereas in **C**, patient C (female, 69 y.) exhibited a high MPG with a comparably low TKE. In patient A, a large inlet of the brachiocephalic artery leads to increased TKE values at the site of flow separation. In contrast to patients B and C, patient A exhibited elevated TKE production throughout the aorta because of high velocity gradients. All patients had tricuspid valves, and the ascending aorta of patient A was dilated. The pathlines are restricted to the investigation domain, which is further illustrated by the red line. Videos for all 3 patients can be found in the [Data Supplement](#).

TKE was found to be significantly higher in patients with AS when compared with healthy, age-matched controls. However, no significant or only weak correlations between MRI-based TKE and echocardiographic parameters were detected. The poor interdependence between TKE metrics and MPG or ELI in AS patients implies that TKE captures other AS characteristics than echocardiography. Indeed, peak TKE and normalized TKE_{sys} were found to be significantly influenced by aortic and valvular morphology.

In the study population with dilated AAO, TKE was significantly increased, whereas MPG was significantly lower. A theoretical approach to explain this observation is given by the Borda–Carnot equation³⁰ which is used in fluid dynamics to describe energy losses of a fluid caused by sudden flow expansion as seen in AS. The increased energy loss is related to a higher degree of turbulent flow mixing at the borders of the jet, thereby resulting in higher TKE levels. This hypothesis is supported by the previous experimental observation of

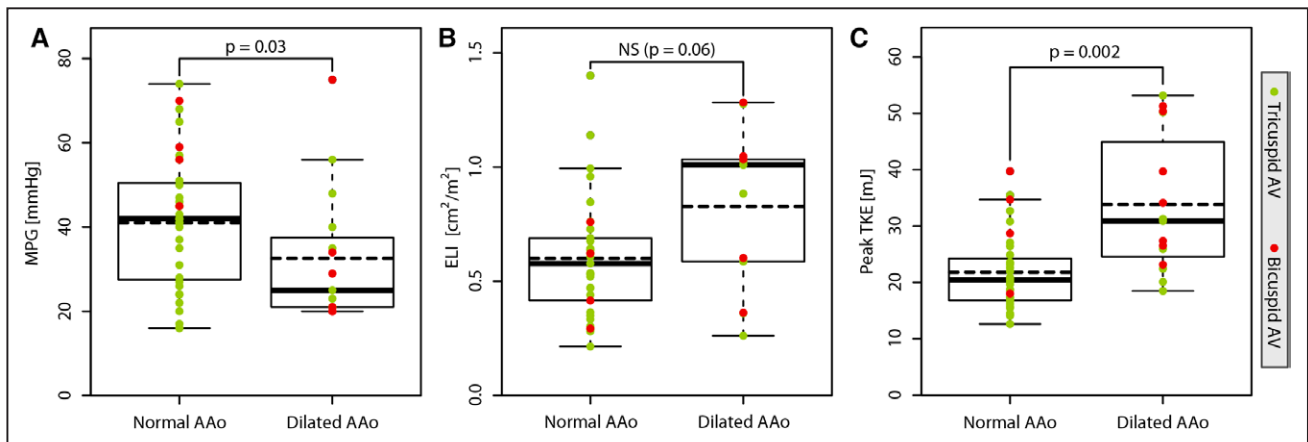


Figure 3. Comparison of mean pressure gradient (MPG; **A**), energy loss index (ELI; **B**), and peak turbulent kinetic energy (TKE; **C**) in patients with normal and dilated ascending aorta (AAo). The green and red dots represent the data points attributed to subjects with tricuspid and bicuspid aortic valves, respectively. Mean values are displayed as dashed horizontal lines. The MPG is significantly lower in the population with dilated AAO. If, however, the varying pressure recovery because of different AAO diameters is factored in by determining ELI, no significant difference can be observed. TKE values indicate a significantly higher energy loss in patients with dilated aorta.

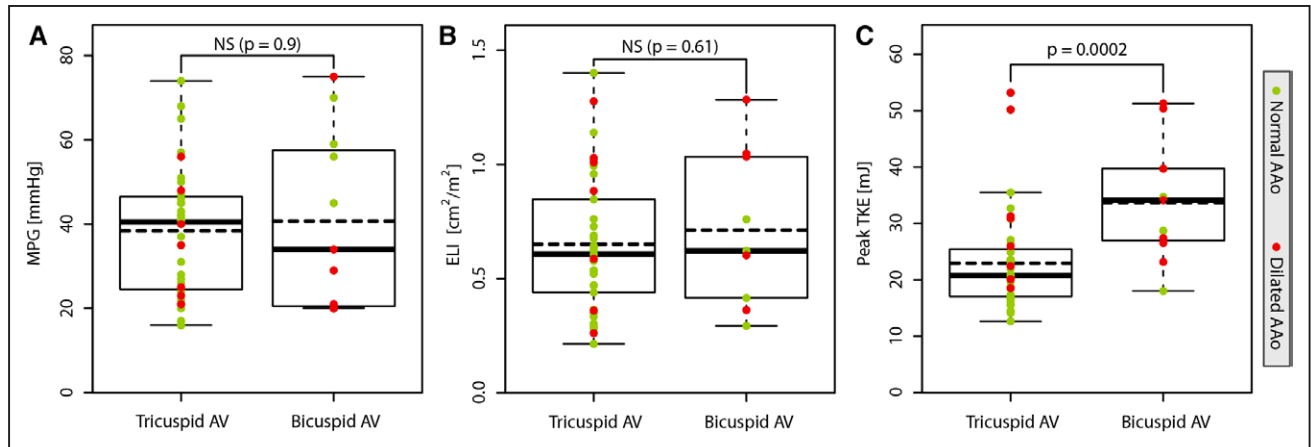


Figure 4. Mean pressure gradient (MPG; **A**), energy loss index (ELI; **B**), and peak turbulent kinetic energy (TKE; **C**) in patients with tricuspid and bicuspid aortic valves (BAV). Mean values are displayed as dashed horizontal lines. Whereas no significant differences are found for MPG and ELI, peak TKE values are significantly elevated in BAV patients. Highest Peak TKE values were found in patients with BAV and aortic dilatation.

an increased amount of vortices in patients with aortic dilatation,³¹ which may translate into higher TKE with the elevated flow velocities accompanying AS. To account for the diameter of the AAO in the echocardiographic assessment, we computed the ELI for our study population as proposed by Garcia et al.⁹ Although MPG was lower in the group with dilated AAO, ELI showed no significant difference in predicted energy loss between patients with dilated and normal AAO.

Furthermore, we found that TKE is elevated in patients with bicuspid aortic valves. Using fluid dynamics, a previous study revealed that the degree of pressure recovery depends on the angle of the jet relative to the axis of the vessel.³² As bicuspid valves often cause a more pronounced flow eccentricity and more deflected jet angles, higher energy losses can be expected when compared with flow downstream of tricuspid valves. Although patients with bicuspid valves often have a dilated aorta, no significant interaction of TKE values for valve morphology and AAO diameter could be found in our study population. Interestingly, a recent study by Schnell et al³³ revealed that relatives of patients with bicuspid valves exhibit altered aortic shape and increased vortical flow pattern

in the absence of valvular disease or aortic dilatation. This finding implies that also non-valve-related effects of aortic shape with impact on aortic flow patterns may influence TKE in bicuspid patients.

The visualization of TKE in the aortic arch of individual patients confirms that energy losses do not only occur directly distal to the stenotic valve. Depending on the interaction of valvular anatomy, aortic geometry, and luminal flow, patient-specific patterns of energy loss can be observed. In contrast, the echocardiographic MPG assesses AS severity only by measuring the jet velocity at the vena contracta. Likewise an extended echocardiographic evaluation by factoring in the aortic diameter at the STJ like the ELI is limited because it does not account for varying jet characteristics or aortic dilatation distal to the STJ.

Elevated levels of TKE in AS patients and a good correlation between calculated irreversible pressure loss and TKE have previously been shown in a pilot study by Dyverfeldt et al²⁰ that included 14 AS patients and 4 healthy controls. However, this study did not investigate correlation between TKE and standard echocardiographic parameters and influencing factors of TKE.

In our study cohort of AS patients, the comparison between MRI and echocardiography demonstrated that two thirds of the population were congruently classified with either mildly or moderately elevated MPG (<40 mm Hg) and TKE or severe elevation of both parameters. The remaining third of the AS patients exhibited a discrepancy between the MPG and the energy loss, while in most cases, TKE under-rated AS severity compared with MPG. The ability of 4D flow MRI to capture patient-specific flow patterns might contribute to the discrepancies and to the lack of correlation with echocardiography. Therefore, TKE might provide complementary information to the echocardiographic examination of AS, helping to distinguish within the heterogeneous population of patients with moderate to severe AS. In particular in patients with discrepant echocardiographic findings on MPG and AVA, in patients who do not qualify for exercise testing to reveal exercise-induced symptoms, or in patients who have confounding diseases so

Table 3. Results From the 2-Way ANOVA Analysis for Valve and Aortic Geometries in All AS Patients

	Dilated AAO	Bicuspid AV	Normal AAO/AV	Interaction, P Value
MPG, mmHg	33±16*	41±21	39±15	0.066
ELI, cm ² /m ²	0.83±0.35	0.71±0.34	0.61±0.27	0.553
Peak TKE, mJ	34±12†	34±11‡	20.8±5.5	0.353
Total TKE _{sys} , mJ	116±41†	122±41‡	73±23	0.116
Normalized TKE _{sys} , mJ/mL	1.53±0.8	1.62±0.63†	1.03±0.31	0.226

Data are mean±SD. Significance level vs patients with a normal geometry. AAO indicates ascending aorta; AS, aortic stenosis; AV, aortic valve; ELI, energy loss index; MPG, mean pressure gradient; and TKE, turbulent kinetic energy.

* $P < 0.05$.

† $P < 0.01$.

‡ $P < 0.001$.

that symptoms cannot unambiguously be attributed to AS, TKE may serve as surrogate for the hemodynamic severity of AS. Consequently, our findings warrant future research to investigate the clinical implications of TKE measures. At first, a subsequent study may correlate TKE with functional or laboratory tests that are known to predict outcome in patients with AS like peak oxygen consumption or N-terminal BNP.^{34,35} Ultimately, a longitudinal trial to investigate the predictive value of TKE for symptom-free survival will be needed to determine the future role of TKE in risk reclassification and therapeutic decision-making for patients with AS.

Study Limitations

TKE measurements using phase-contrast MRI are inherently sensitive to the selection of the encoding velocity. This was mitigated by using a multipoint approach with 3 different encoding velocities per direction, extending the dynamic range of the TKE assessment.

Viscous losses not related to turbulence also contribute to the total energy loss but have not been evaluated in this study. However, previous studies¹⁹ showed that losses because of TKE exceeded nonturbulent viscous losses by a factor of 4 to 5 for moderate to severe stenosis, and currently used spatial resolutions are not sufficient for accurate viscous loss estimation.

Because of the limited spatial resolution of 4D flow MRI data, velocity gradients at the vessel wall were excluded in the analysis because they would result in erroneous TKE parameters because of partial volume effects. To this end, care was taken during the semiautomatic vessel segmentation steps not to include the vessel wall. However, inclusion of partial volume voxels in the analysis cannot be entirely ruled out. In patients with eccentric jets, high TKE values are also found close to the wall, which in turn are excluded from the analysis. Their impact on the TKE parameters, however, should be negligible because they only constitute a minor fraction of the volume of interest.

In summary, TKE allows to quantify the influence of valve morphology and AAO geometry on the hemodynamic burden of AS. Elevated TKE levels, noninvasively quantified by 4D flow MRI, imply higher energy losses associated with bicuspid aortic valves and dilated AAO geometries that are not assessable by current echocardiographic measures.

Sources of Funding

This work was supported by grants from the Swiss National Science Foundation (CR23I3-144218) and the National Competence Center in Biomedical Imaging Switzerland and by an unrestricted grant from Bayer Health Care, Zurich, Switzerland.

Disclosures

None.

References

- Iung B, Baron G, Butchart EG, Delahaye F, Gohlke-Bärwolf C, Levang OW, Tornos P, Vanoverschelde JL, Vermeer F, Boersma E, Ravaut P, Vahanian A. A prospective survey of patients with valvular heart disease in Europe: The Euro Heart Survey on Valvular Heart Disease. *Eur Heart J*. 2003;24:1231–1243.
- Nkomo VT, Gardin JM, Skelton TN, Gottdiener JS, Scott CG, Enriquez-Sarano M. Burden of valvular heart diseases: a population-based study. *Lancet*. 2006;368:1005–1011. doi: 10.1016/S0140-6736(06)69208-8.
- Vahanian A, Alfieri O, Andreotti F, Antunes MJ, Baron-Esquivias G, Baumgartner H, Borger MA, Carrel TP, De Bonis M, Evangelista A, Falk V, Jung B, Lancellotti P, Pierard L, Price S, Schafers HJ, Schuler G, Stepinska J, Swedberg K, Takkenberg J, Von Oppell UO, Windecker S, Zamorano JL, Zembala M. Guidelines on the management of valvular heart disease (version 2012). *Eur Heart J*. 2012;33:2451–2496.
- Nishimura RA, Otto CM, Bonow RO, Carabello BA, Erwin JP III, Guyton RA, O’Gara PT, Ruiz CE, Skubas NJ, Sorajja P, Sundt TM III, Thomas JD; ACC/AHA Task Force Members. 2014 AHA/ACC Guideline for the Management of Patients With Valvular Heart Disease: a report of the American College of Cardiology/American Heart Association Task Force on Practice Guidelines. *Circulation*. 2014;129:e521–e643. doi: 10.1161/CIR.0000000000000031.
- Stähli BE, Abouelnour A, Nguyen TD, Vecchiati A, Maier W, Lüscher TF, Frauenfelder T, Tanner FC. Impact of three-dimensional imaging and pressure recovery on echocardiographic evaluation of severe aortic stenosis: a pilot study. *Echocardiography*. 2014;31:1006–1016. doi: 10.1111/echo.12509.
- Kamperidis V, van Rosendaal PJ, Katsanos S, van der Kley F, Regeer M, Al Amri I, Sianos G, Marsan NA, Delgado V, Bax JJ. Low gradient severe aortic stenosis with preserved ejection fraction: reclassification of severity by fusion of Doppler and computed tomographic data. *Eur Heart J*. 2015;36:2087–2096. doi: 10.1093/eurheartj/ehv188.
- Chin CW, Khaw HJ, Luo E, Tan S, White AC, Newby DE, Dweck MR. Echocardiography underestimates stroke volume and aortic valve area: implications for patients with small-area low-gradient aortic stenosis. *Can J Cardiol*. 2014;30:1064–1072. doi: 10.1016/j.cjca.2014.04.021.
- Clavel MA, Dumesnil JG, Pibarot P. Discordant grading of aortic stenosis using echocardiography and what it means: new insights from magnetic resonance imaging. *Can J Cardiol*. 2014;30:959–961. doi: 10.1016/j.cjca.2014.06.007.
- Garcia D, Pibarot P, Dumesnil JG, Sakr F, Durand LG. Assessment of aortic valve stenosis severity: a new index based on the energy loss concept. *Circulation*. 2000;101:765–771.
- Garcia D, Dumesnil JG, Durand LG, Kadem L, Pibarot P. Discrepancies between catheter and Doppler estimates of valve effective orifice area can be predicted from the pressure recovery phenomenon: practical implications with regard to quantification of aortic stenosis severity. *J Am Coll Cardiol*. 2003;41:435–442.
- Bahlmann E, Gerds E, Cramariuc D, Gohlke-Baerwolf C, Nienaber CA, Wachtell K, Seifert R, Chambers JB, Kuck KH, Ray S. Prognostic value of energy loss index in asymptomatic aortic stenosis. *Circulation*. 2013;127:1149–1156. doi: 10.1161/CIRCULATIONAHA.112.078857.
- Baumgartner H, Hung J, Bermejo J, Chambers JB, Evangelista A, Griffin BP, Iung B, Otto CM, Pellikka PA, Quinones M. Echocardiographic assessment of valve stenosis: EAE/ASE recommendations for clinical practice. *J Am Soc Echocardiogr*. 2009;22:1–23; quiz 101–102.
- von Knobelsdorff-Brenkenhoff F, Karunaharamoorthy A, Trauzeddel RF, Barker AJ, Blaszczyk E, Markl M, Schulz-Menger J. Evaluation of aortic blood flow and wall shear stress in aortic stenosis and its association with left ventricular remodeling. *Circ Cardiovasc Imaging*. 2016;9:e004038. doi: 10.1161/CIRCIMAGING.115.004038.
- Firmin DN, Gatehouse PD, Konrad JP, Yang GZ, Kilner PJ, Longmore DB. Rapid 7-dimensional imaging of pulsatile flow. *Comput Cardiol*. 1993;14:353–356.
- Wigström L, Sjöqvist L, Wranne B. Temporally resolved 3D phase-contrast imaging. *Magn Reson Med*. 1996;36:800–803.
- Buonocore MH. Visualizing blood flow patterns using streamlines, arrows, and particle paths. *Magn Reson Med*. 1998;40:210–226.
- Dyverfeldt P, Kvitting JP, Sigfridsson A, Engvall J, Bolger AF, Ebbens T. Assessment of fluctuating velocities in disturbed cardiovascular blood flow: *in vivo* feasibility of generalized phase-contrast MRI. *J Magn Reson Imaging*. 2008;28:655–663. doi: 10.1002/jmri.21475.
- Barker AJ, van Ooij P, Bandi K, Garcia J, Albaghdadi M, McCarthy P, Bonow RO, Carr J, Collins J, Malaisrie SC, Markl M. Viscous energy loss in the presence of abnormal aortic flow. *Magn Reson Med*. 2014;72:620–628. doi: 10.1002/mrm.24962.
- Binter C, Gülan U, Holzner M, Kozerke S. On the accuracy of viscous and turbulent loss quantification in stenotic aortic flow using phase-contrast MRI. *Magn Reson Med*. 2016;76:191–196. doi: 10.1002/mrm.25862.
- Dyverfeldt P, Hope MD, Tseng EE, Saloner D. Magnetic resonance measurement of turbulent kinetic energy for the estimation of irreversible pressure loss in aortic stenosis. *JACC Cardiovasc Imaging*. 2013;6:64–71. doi: 10.1016/j.jcmg.2012.07.017.

21. Ha H, Kim GB, Kweon J, Huh HK, Lee SJ, Koo HJ, Kang JW, Lim TH, Kim DH, Kim YH, Kim N, Yang DH. Turbulent kinetic energy measurement using phase contrast MRI for estimating the post-stenotic pressure drop: *in vitro* validation and clinical application. *PLoS One*. 2016;11:e0151540. doi: 10.1371/journal.pone.0151540.
22. Kramer CM, Barkhausen J, Flamm SD, Kim RJ, Nagel E; Society for Cardiovascular Magnetic Resonance Board of Trustees Task Force on Standardized Protocols. Standardized cardiovascular magnetic resonance (CMR) protocols 2013 update. *J Cardiovasc Magn Reson*. 2013;15:91. doi: 10.1186/1532-429X-15-91.
23. Binter C, Knobloch V, Manka R, Sigfridsson A, Kozzerke S. Bayesian multipoint velocity encoding for concurrent flow and turbulence mapping. *Magn Reson Med*. 2013;69:1337–1345. doi: 10.1002/mrm.24370.
24. Knobloch V, Binter C, Kurtcuoglu V, Kozzerke S. Arterial, venous, and cerebrospinal fluid flow: simultaneous assessment with Bayesian multipoint velocity-encoded MR imaging. *Radiology*. 2014;270:566–573. doi: 10.1148/radiol.13130840.
25. Pedersen H, Kozzerke S, Ringgaard S, Nehrke K, Kim WY. k-t PCA: temporally constrained k-t BLAST reconstruction using principal component analysis. *Magn Reson Med*. 2009;62:706–716. doi: 10.1002/mrm.22052.
26. Voelker W, Reul H, Stelzer T, Schmidt A, Karsch KR. Pressure recovery in aortic stenosis: an *in vitro* study in a pulsatile flow model. *J Am Coll Cardiol*. 1992;20:1585–1593.
27. Niederberger J, Schima H, Maurer G, Baumgartner H. Importance of pressure recovery for the assessment of aortic stenosis by Doppler ultrasound. Role of aortic size, aortic valve area, and direction of the stenotic jet *in vitro*. *Circulation*. 1996;94:1934–1940.
28. Richards KE, Deserranno D, Donal E, Greenberg NL, Thomas JD, Garcia MJ. Influence of structural geometry on the severity of bicuspid aortic stenosis. *Am J Physiol Heart Circ Physiol*. 2004;287:H1410–H1416. doi: 10.1152/ajpheart.00264.2003.
29. Walker PG, Cranney GB, Scheidegger MB, Waseleski G, Pohost GM, Yoganathan AP. Semiautomated method for noise reduction and background phase error correction in MR phase velocity data. *J Magn Reson Imaging*. 1993;3:521–530.
30. Douglas JF. *Fluid Mechanics*. Harlow, United Kingdom: Prentice Hall; 2005.
31. Frydrychowicz A, Berger A, Munoz Del Rio A, Russe MF, Bock J, Harloff A, Markl M. Interdependencies of aortic arch secondary flow patterns, geometry, and age analysed by 4-dimensional phase contrast magnetic resonance imaging at 3 Tesla. *Eur Radiol*. 2012;22:1122–1130. doi: 10.1007/s00330-011-2353-6.
32. Clark C. Energy losses in flow through stenosed valves. *J Biomech*. 1979;12:737–746.
33. Schnell S, Smith DA, Barker AJ, Entezari P, Honarmand AR, Carr ML, Malaisrie SC, McCarthy PM, Collins J, Carr JC, Markl M. Altered aortic shape in bicuspid aortic valve relatives influences blood flow patterns. *Eur Heart J Cardiovasc Imaging*. 2016;17:1239–1247. doi: 10.1093/ehjci/jew149.
34. Dhoble A, Enriquez-Sarano M, Kopecky SL, Abdelmoneim SS, Cruz P, Thomas RJ, Allison TG. Cardiopulmonary responses to exercise and its utility in patients with aortic stenosis. *Am J Cardiol*. 2014;113:1711–1716. doi: 10.1016/j.amjcard.2014.02.027.
35. Bergler-Klein J, Klaar U, Heger M, Rosenhek R, Mundigler G, Gabriel H, Binder T, Pacher R, Maurer G, Baumgartner H. Natriuretic peptides predict symptom-free survival and postoperative outcome in severe aortic stenosis. *Circulation*. 2004;109:2302–2308. doi: 10.1161/01.CIR.0000126825.50903.18.

CLINICAL PERSPECTIVE

Risk stratification and therapeutic decisions in aortic stenosis (AS) are primarily based on echocardiography and the presentation of symptoms. Echocardiography, however, leads to discordant findings between mean pressure gradient and aortic valve area in a third of patients with moderate or severe AS and has only limited potential to account for hemodynamic effects, such as poststenotic pressure recovery. On the other hand, attributing symptoms unambiguously to AS is often impaired by patients' limited exercise capability or confounding diseases, such as coronary artery disease. Those limitations stress the need for improved diagnostics for AS patients. Four-dimensional flow magnetic resonance imaging allows to assess the turbulent kinetic energy (TKE)—the energy stored and largely lost in the flow disturbance caused by AS—which may serve as a surrogate parameter for the additional myocardial workload. In this study, we therefore investigated the occurrence of TKE in patients with AS in comparison to echocardiographic findings. AS patients had significantly higher TKE than healthy controls, whereas, within the group of AS patients, TKE and echocardiographic mean pressure gradient showed no significant correlation. In particular, in patients with aortic dilation or bicuspid aortic valves, TKE but not mean pressure gradient was significantly elevated. These results imply that TKE can capture hemodynamic effects of valve morphology and aortic geometry on the energy loss caused by AS that are not assessable with echocardiography. Our findings should stimulate future longitudinal trials to determine the predictive value of TKE in the risk stratification of AS patients.

Turbulent Kinetic Energy Assessed by Multipoint 4-Dimensional Flow Magnetic Resonance Imaging Provides Additional Information Relative to Echocardiography for the Determination of Aortic Stenosis Severity

Christian Binter, Alexander Gotschy, Simon H. Sündermann, Michelle Frank, Felix C. Tanner, Thomas F. Lüscher, Robert Manka and Sebastian Kozerke

Circ Cardiovasc Imaging. 2017;10:

doi: 10.1161/CIRCIMAGING.116.005486

Circulation: Cardiovascular Imaging is published by the American Heart Association, 7272 Greenville Avenue, Dallas, TX 75231

Copyright © 2017 American Heart Association, Inc. All rights reserved.

Print ISSN: 1941-9651. Online ISSN: 1942-0080

The online version of this article, along with updated information and services, is located on the World Wide Web at:

<http://circimaging.ahajournals.org/content/10/6/e005486>

Data Supplement (unedited) at:

<http://circimaging.ahajournals.org/content/suppl/2017/06/13/CIRCIMAGING.116.005486.DC1>

Permissions: Requests for permissions to reproduce figures, tables, or portions of articles originally published in *Circulation: Cardiovascular Imaging* can be obtained via RightsLink, a service of the Copyright Clearance Center, not the Editorial Office. Once the online version of the published article for which permission is being requested is located, click Request Permissions in the middle column of the Web page under Services. Further information about this process is available in the [Permissions and Rights Question and Answer](#) document.

Reprints: Information about reprints can be found online at:
<http://www.lww.com/reprints>

Subscriptions: Information about subscribing to *Circulation: Cardiovascular Imaging* is online at:
<http://circimaging.ahajournals.org/subscriptions/>

**Turbulent Kinetic Energy Assessed by Multipoint 4D Flow MRI Provides
Additional Information Relative to Echocardiography for the
Determination of Aortic Stenosis Severity**

SUPPLEMENTAL MATERIAL

Christian Binter, PhD¹; Alexander Gotschy, MD, MSc^{1,2,3}; Simon H. Sündermann, MD⁴; Michelle Frank, MD²; Felix C. Tanner, MD²; Thomas F. Lüscher, MD²; Robert Manka, MD^{2,5}; and Sebastian Kozerke, PhD^{1,6}

¹Institute for Biomedical Engineering, University and ETH Zurich, Zurich, Switzerland;
²Department of Cardiology, University Heart Center, University Hospital Zurich, Zurich, Switzerland; ³Division of Internal Medicine, University Hospital Zurich, Zurich, Switzerland;
⁴Department of Cardiothoracic and Vascular Surgery, Deutsches Herzzentrum Berlin, Berlin, Germany; ⁵Institute of Diagnostic and Interventional Radiology, University Hospital Zurich, Zurich, Switzerland; ⁶Imaging Sciences and Biomedical Engineering, King's College London, London, United Kingdom

C.B. and A.G. share first authorship.

Short Title: Turbulent Kinetic Energy in Aortic Stenosis

Address for Correspondence:

Sebastian Kozerke, PhD
Institute for Biomedical Engineering
University and ETH Zurich
Gloriastrasse 35
8092 Zurich, SWITZERLAND
Tel.: + 41 44 632 3549
Fax: + 41 44 632 1193
Email: kozerke@biomed.ee.ethz.ch

Supplemental Methods

TKE determination by Multipoint 4D Flow MRI

The signal model for Phase-Contrast MRI as described by Dyverfeldt et al.¹ relates the intravoxel velocity standard deviation σ to attenuation of the signal magnitude S depending on the encoding velocity $VENC$ according to:

$$|S(k_v)| = |S_0| e^{-\frac{\sigma^2 k_v^2}{2}} \quad \text{with} \quad k_v = \frac{\pi}{VENC} \quad \text{Eq. A1}$$

Because of the dependency of the signal on k_v^2 and σ^2 an estimate for the expected TKE is required for scans with a single encoding velocity to achieve maximum sensitivity, and k_v has to be adjusted accordingly. The optimum k_v for an estimated velocity standard deviation σ_{est} is given by $|k_v| = 1/\sigma_{\text{est}}$ ¹. Using multiple encoding velocities, this estimation is no longer necessary, as the VENCs employed in this study (50, 150 and 450 cm/s) cover isotropic TKE values in the range of approximately 40 and 3000 J/m³. By employing Bayesian parameter estimation² all encoding velocities are taken into account for a joint determination of σ and mean velocity v , yielding a probability distribution. This is achieved by a decomposition of the complex-valued signal into two projections onto the signal model which is given by

$$S(k_v) = S_0 e^{-\frac{\sigma^2 k_v^2}{2}} e^{-ivk_v} \quad \text{Eq. A2}$$

For every obtained VENC data point, all values for v and σ are assigned a certain probability. In this study three VENC values were acquired in each direction and the resulting probabilities combined to obtain $P(\{v, \sigma\} | D, I)$ – the posterior probability for v and σ given the measured data D and the model I . The Bayesian analysis implicitly weights the contributions of the different VENCs. For example, measurements with little signal contribute less to the probability of the mean velocity. A mathematical description and visualization of the Bayesian process can also be found in³.

The Bayesian method allows capturing a wide range of velocities without the need for velocity anti-aliasing while simultaneously providing the data necessary for TKE calculation.

Calculation of TKE derived parameters

Peak TKE, Total TKE_{sys} and Normalized TKE_{sys} were obtained by integrating TKE values over all n_{IV} voxels in the investigation volume as depicted in Fig. 2. Peak TKE describes the kinetic energy stored in velocity fluctuations during peak systole (t_{peak}):

$$Peak\ TKE\ [mJ] = \sum_{x=1}^{n_{IV}} TKE(x, t_{peak}) \cdot V_{voxel} \quad Eq. A2$$

where V_{voxel} denotes the voxel volume. Total TKE_{sys}, the total dissipated energy during systole, is obtained by integrating TKE over all n_{sys} systolic timeframes:

$$Total\ TKE_{sys}\ [mJ] = \sum_{t=1}^{n_{sys}} \sum_{x=1}^{n_{IV}} TKE(x, t) \cdot V_{voxel} \cdot \frac{t_{frame}}{t_{turnover}} \quad Eq. A3$$

where t_{frame} is the temporal resolution and $t_{turnover}$ is the turnover time. This turnover rate describes the time from TKE production to dissipation. In-vitro experiments have shown $t_{turnover}$ to be 70 ms for moderate to severe stenosis. By including the turnover rate, a physically meaningful parameter (in mJ rather than mJs) is obtained.

Normalized TKE_{sys} as described in Eq. 2 relates Total TKE_{sys} to the stroke volume. The SV is used as a surrogate measure for the physiological workload of the heart, thereby making the increased load as determined by TKE comparable between patients.

Reproducibility

The volume of interest was segmented semi-automatically. A mask was calculated based on the temporal properties of the velocities in the volume and provided to the readers as a basis. The readers could then adapt the volume of interest manually based on the velocities and TKE

values. This approach was chosen to ensure consistent segmentation. Reproducibility was analysed and presented at the ISMRM Annual Meeting 2014 (Abstract #2477), where the analysis of intra- and inter-observer variability yielded mean differences of $3.4\pm 3.3\%$ and $11.8\pm 6.8\%$, respectively.

Spatiotemporal undersampling and SNR

Compared to frame-by-frame undersampling, spatiotemporal undersampling techniques such as k-t PCA exhibit a less pronounced decrease in signal-to-noise ratio (SNR) with increasing undersampling factor. A g_x^{avg} -factor analysis⁴ showed comparable g-factors for 5-fold and 7-fold reduction, indicating that the SNR decrease for higher undersampling factors is approximated by the square root of the relative increase of the undersampling factor. Due to the multiple encoding velocities of the Bayesian multipoint approach, the noise in the computed velocity field will also be lower than in conventional PC-MRI acquisitions with the same undersampling factor².

While the effect on noise is thus limited, increased acceleration results in temporal smoothing, leading to underestimation of peak velocities and flow rates in the case of accelerated Phase-Contrast flow measurements. Work by Giese et al.⁵ showed a limit of 5-fold undersampling for k-t SENSE, and a limit above 10-fold for k-t PCA.

1. Dyverfeldt P, Sigfridsson A, Kvitting JP, Ebbers T. Quantification of intravoxel velocity standard deviation and turbulence intensity by generalizing phase-contrast MRI. *Magn Reson Med.* 2006;56:850-858
2. Binter C, Knobloch V, Manka R, Sigfridsson A, Kozerke S. Bayesian multipoint velocity encoding for concurrent flow and turbulence mapping. *Magn Reson Med.* 2013;69:1337-1345
3. Knobloch V, Binter C, Gulan U, Sigfridsson A, Holzner M, Luthi B, Kozerke S. Mapping mean and fluctuating velocities by bayesian multipoint mr velocity encoding-validation against 3d particle tracking velocimetry. *Magn Reson Med.* 2014;71:1405-1415
4. Binter C, Ramb R, Jung B, Kozerke S. A g-factor metric for k-t sense and k-t PCA based parallel imaging. *Magn Reson Med.* 2016;75:562-571
5. Giese D, Schaeffter T, Kozerke S. Highly undersampled phase-contrast flow measurements using compartment-based k-t principal component analysis. *Magn Reson Med.* 2013;69:434-443

Supplementary Video Captions

SupplVideo_PatientA.mpg:

Pathlines of Patient A with a dilated ascending aorta and high TKE values (see Fig. 2).

SupplVideo_PatientB.mpg - Pathlines of Patient B with similar transvalvular velocities compared to Patient A, but lower overall TKE levels (see Fig. 2).

SupplVideo_PatientC.mpg - Pathlines of Patient C, exhibiting high velocities (MPG 74 mmHg) but limited TKE values (see Fig. 2).